



SENSITIVITY ANALYSIS OF FUEL-CLADDING DEBONDING OF HIGH BURNUP SPENT PWR FUEL SUBJECTED TO DRY STORAGE AND TRANSPORTATION ACCIDENTS

KEITH P. WALDROP

¹*Electric Power Research Institute,
CA-94304 Palo Alto - USA*

ANH T. MAI AND JOSEPH Y. R. RASHID

*Structural Integrity Associates, Inc.,
9710 Scranton Road, CA-92121 San Diego - USA*

ABSTRACT

Recent studies have estimated that the peak cladding temperature (PCT) of any spent fuel loaded in dry storage casks to date in the US is lower than the regulatory limit of 400°C, closer to 325°C. Also, there is prevailing evidence that fuel cladding bonding is a characteristic of high burnup spent fuel, which minimizes hydride reorientation and makes fuel rods highly resistant to failure under drop accidents. This paper investigates three aspects of fuel-cladding bonding in high burnup spent fuel under dry storage conditions: the effect of fuel-cladding bonding on cladding hoop stress and hydrides reorientation considering the more realistic PCTs of 350°C and 300°C, the magnitude of fuel partial bonding that simulates the open gap condition and exploring through sensitivity analysis the conditions under which pellet-cladding bonding is likely to break and potential consequences.

For the fuel-cladding bonded condition at lower PCTs than the 400°C case, the cladding hoop stress exhibits low to moderate relaxation because of the reduced creep rate for the PCTs of 350°C and 300°C. Because the hoop stress remains relatively high, radial hydrides concentration is lower than the unbonded condition but higher than the 400°C PCT case. The results also show varied sensitivity to fuel cracking configuration, with low sensitivity for the predominantly typical cracking pattern consisting of radial cracks only, but high sensitivity to fuel with circumferential cracks, which generally occur during shutdown from relatively high-power levels. For the latter case, the cladding hoop stress is at or below the hydride reorientation threshold. The sensitivity analysis investigating the conditions under which pellet-cladding bonding is likely to break revealed that the bond remains intact, and instead secondary circumferential cracks are formed in the fuel pellets.

1. Introduction

A limited scope analysis to evaluate the effect of fuel-cladding bonding on cladding hoop stress and potential hydride reorientation during dry storage was described in a 2018 Top Fuel paper [1] and an EPRI report [2]. Fuel bonding was introduced at cold conditions at 40°C just before the start of vacuum drying to a maximum temperature of 400°C. The loading consisted of differential thermal expansion and internal gas pressure; the latter was assumed to be contained in the fuel rod void volume which consisted of fuel cracks shown in the finite element grid (Figure 1A) and in fuel matrix open porosity. In contrast, for the case of low burnup unbonded fuel, the loading on the cladding is due to internal gas pressure only directly applied to the cladding as an empty tube.



The analysis results indicate that the cladding hoop stress in the bonded fuel can be significantly lower than the unbonded case, which would result in much reduced radial hydride concentration. Figure 1 from Ref. [1] shows stress results for a representative case with typical fuel cracking pattern. As shown in the figure, high (29.6 MPa) compressive radial stress in the pellet (Figure 1A) coincides with high (130 MPa) tensile hoop stress in the cladding (Figure 1B). Figure 1C shows cladding hoop stress relaxed within 60 days from 130 MPa to 26.1 MPa; note that at stress concentration points at pellet cracks stress relaxation is smaller, changing from ~95 MPa to ~68 MPa, but is confined to very narrow sections of the order of cladding thickness. Noting from Figure 1B, the flow of hydrogen during vacuum drying is into the narrow sections from the adjacent material but is reversed during stress relaxation as indicated by the stress pattern in Figure 1C. As the temperature continues to decrease during dry storage, hydride precipitation and reorientation starts to occur and remains confined in the cladding sections between pellet radial cracks away from pellet cracks.

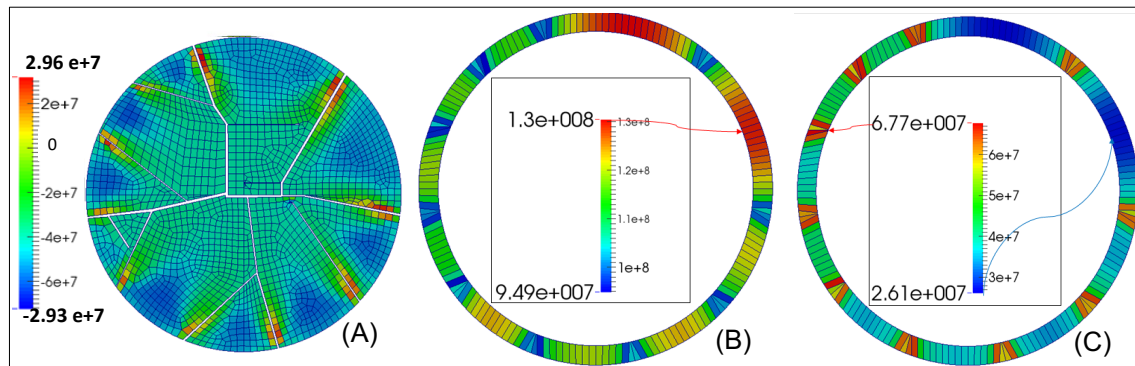


Figure 1. Stress distribution in bonded fuel: (A) and (B) Radial stress in the pellet and hoop stress in the cladding, respectively, at the maximum vacuum drying temperature of 400°C; (C) Cladding hoop stress after 60 days stress relaxation.

The scoping analysis results discussed above encouraged conducting further studies [3] to determine the full attributes of fuel-cladding bonding, which is assumed to develop gradually at a burnup level sometime after reaching 45 GWD/MTU, the designated onset of the high-burnup phenomenon. The importance of fuel-cladding bonding to spent fuel behaviour under dry storage and transportation conditions is reflected in two ways: (a) its effect on cladding hoop stress which governs the magnitude of radial hydrides that can potentially form during dry storage, and (b) its effect on cladding resistance to failure under pinch loading and bending loading experienced in drop accidents. The presence and extent of fuel-cladding bonding determines which cladding failure mode is of greater concern: cladding failure due to pinch loading, which is highly sensitive to radial hydrides, or cladding failure by axial bending, which is unaffected by radial hydrides. This invokes a two-part question: can the beneficial effects of fuel-cladding bonding be neutralized by bond breaking during wet or dry storage, and if the bond breaks, how wide does an unbonded arc length have to be to make the cladding hoop stress equivalent to pressurized empty tube, thereby maximizing the effects of radial hydrides. The first part of the question is addressed in a sensitivity analysis in Section 3, and the answer to the second part is presented in Section 2.

2. Analysis of Partial Debonding

Potential impact of bond breaking on spent fuel behavior during dry storage and transportation is measured by the extent of fuel debonding relative to the open gap condition. Three variations of unbonded arc length are imposed on the finite element grid shown in Figure 1A above. Partial debonding was introduced by separating the fuel elements from the cladding elements in regions between pellet cracks. Debonding, if it were to occur, would begin at a pellet crack and could extend along the entire arc length between two pellet cracks. This forces the unbonded arc lengths to conform to the cracking pattern, with

the following approximate lengths: 27 degrees, 52 degrees and 102 degrees. The analysis time history included a period of 60 days for creep and stress relaxation at 400°C starting from the completion of vacuum drying. Figure 2 provides the stress distribution at the completion of the vacuum drying process for the three partial debonding cases analyzed. Cross comparison of the cladding stress patterns in Figure 2 reveals that the cladding hoop stress in the unbonded sections, (blue color) is nearly the same for all three arc lengths with a value of ~85 MPa. This is indicative of pressurized tube behavior which is not subject to relaxation; this is confirmed by Figure 3 which shows nearly the same stress magnitude in the unbonded sections after 60-day stress relaxation. The above results indicate that an unbonded section of about 7.5% of the cladding circumference appears to closely simulate empty tube behavior, as illustrated by the 27-degree arc length case.

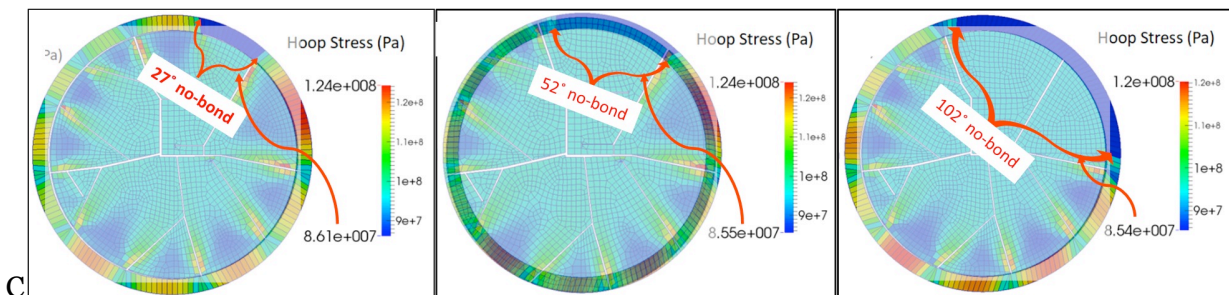


Figure 2. Hoop stress distribution at the completion of vacuum drying at 400°C.

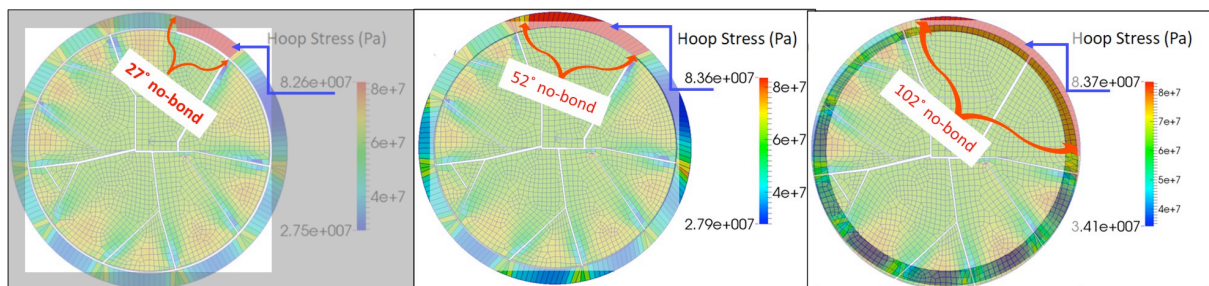


Figure 3. Hoop stress distribution at the end of 60-day relaxation at 400°C.

2.1 Implication for Hydride Reorientation

Experience with defueling high burnup fuel rods for post-irradiation examination consistently indicate that significant mechanical effort had to be applied. The 27-degree unbonded sector is not based on data but is a hypothetical case intended to provide a priori answer to the what-if question. The likelihood of such hypothetical case existing is further diminished by the fact that the fuel-cladding bond is highly resistant to breaking as will be shown in Section 5. However, if we must allow for the possible existence of partial debonding to assess its potential impact on radial hydrides formation, it is conservative to assume that about 7.5% of the cladding circumference is unbonded.

Upon the completion of vacuum drying at a storage temperature of 400°C, as used in this analysis, the level and distribution of the hoop stress in the cladding determine the ultimate magnitude and distribution of radial hydrides as they begin to precipitate at ~335°C, which is the precipitation temperature for the initial temperature of 400°C. The cladding hoop stresses depicted in Figure 1C, for the fully bonded condition fall in the range of 26- 60 MPa, with 67 MPa confined to 1-mm wide segments at pellet crack positions, and less than 85 MPa for the partially bonded condition, Figure 3. The 60-67 MPa hoop stress is at or below the hydride

reorientation threshold stress. However, the 85 MPa stress would lead to the formation of radial hydrides, but the affected area of the cladding is limited to the unbonded section. For this to pose a risk to cladding integrity under pinch loading conditions requires the alignment of three conditions with multiplicative probabilities: positioning the unbonded section of the fuel rod in the 12-clock maximum pinch-loading position, in the bottom row of the 17x17 fuel assembly, and in the bottom assembly of a 24-assembly cask.

3. Analysis Methodology for High Burnup Fuel-Cladding Bonding

This section describes a general analysis procedure for PWR fuel emphasizing the effects of fuel-cladding bonding, which develop during high burnup operation, on cladding behavior during spent fuel storage and transportation; in particular, the formation of radial hydrides during long-term storage and their impact on cladding integrity under cask drop accidents. Fuel-cladding bonding phenomenon, as a manifestation of high-burnup operation, acts as a cladding-stress reducing mechanism by shifting the internal gas pressure to fuel cracks away from direct bearing on the cladding. Although fuel bonding concern is related to its effect on hydride reorientation during dry storage, the analysis of the phenomenon must cover the entire time history of the fuel starting from zero burnup through end-of-life power operation, activating fuel-cladding bonding at some burnup level in the high burnup regime, wet storage and extended dry storage. This requires special capabilities that are not usually found in a single fuel performance code, which include the modeling of three behavior regimes: fuel cracking, crack pressurization and multi-regime modeling of fuel-cladding interface. To capture these behavior regimes fully in the present analysis, two fuel performance codes are used, each providing the features that are better suited for the problem: EPRI's Falcon code [6] and DOE/CASL's BISON code [7]. The analysis begins with the Falcon code using a full-length R-Z finite element model of the fuel rod, takes the model through a two-cycle base irradiation power history to reach the maximum licensing burnup level of 62 GWD/MTU, and produces a record of the internal gas pressure history for input to BISON. BISON repeats the analysis with plane-strain R- θ model with discrete cracks depicted in Figure 1A, using the average time history of the same two-cycle base irradiation power, together with the gas pressure history generated by Falcon. As BISON analysis progresses in time it adds the Falcon-generated gas pressure history to the cracks, continues with the analysis to 62 GWD/MTU, activating pellet-cladding bonding after gap closure at a burnup of ~60 GWD/MTU. Fuel-cladding bonding is simulated in the fuel-cladding gap interface with finite elements having the mechanical properties of UO₂ and ZrO₂ material mixture. At the end-of-life burnup the BISON analysis is shutdown to cold zero power followed by a simulation of wet storage at 40°C, and finally vacuum drying to the specified temperature followed by one year of dry storage to allow creep and stress relaxation to occur. The choice of one year instead of longer time is due to the fact that cladding creep during the early period of dry storage is sufficiently fast to achieve steady state condition.

3.1 Analysis Results

The above-described analysis procedure was applied to all three dry storage temperature conditions, 400°C, 350°C and 300°C. Contour plots are presented for stress components of interest, namely: the radial stress in the fuel, which represents the PCMI force; and the hoop stress in the cladding, which governs hydride reorientation. The stress distributions in Figures 4 for 400°C, Figure 5 for 350°C and Figure 6 for 300°C are depicted for the completion of vacuum drying and the end of one-year storage.

All three figures have the same caption except for the temperature; the following description applies to all figures: Stress distribution in bonded fuel; (A) and (B) Radial stress in the pellet and hoop stress in the cladding, respectively, at the maximum vacuum drying temperature; (c) Cladding hoop stress after one year creep and stress relaxation.

It would be instructive to draw a comparison between the cases for cladding hoop stress post vacuum drying. Table 1 lists cladding peak hoop stress for the three temperatures. As shown in the table, the magnitude of stress relaxation varies considerable with temperature. The most interesting comparison is between the 400°C case and the 300°C case, which show almost equal PCMI force, as represented by the maximum compressive radial stress in the fuel, yet the stress reduction in the cladding varies from a factor of 6.5 for the higher temperature to a factor of 1.2 for the lower temperature. As further observation, the hoop stress at the completion of vacuum drying for all three cases, calculated using the end-of-life internal gas pressure from Reference [4], is below the pressurized tube (unbonded) case, as shown in Table 1. However, the one-year results are the stress values to use for evaluating the implication to hydride reorientation. This is discussed in a later section in this paper. The one-year stress reductions for the unbonded cases are caused by the decrease in pressure due to temperature decay.

Table 1. Post-vacuum drying cladding stress in dry storage.

Temperature at t = 0	Stress (MPa) at t = 0		Stress (MPa) at t = 1yr.	
	Bonded	unbonded	Bonded	unbonded
400°C	73.2	85	11.3	82
350°C	73.0	78.6	27.7	76
300°C	62.3	72.4	53.1	70

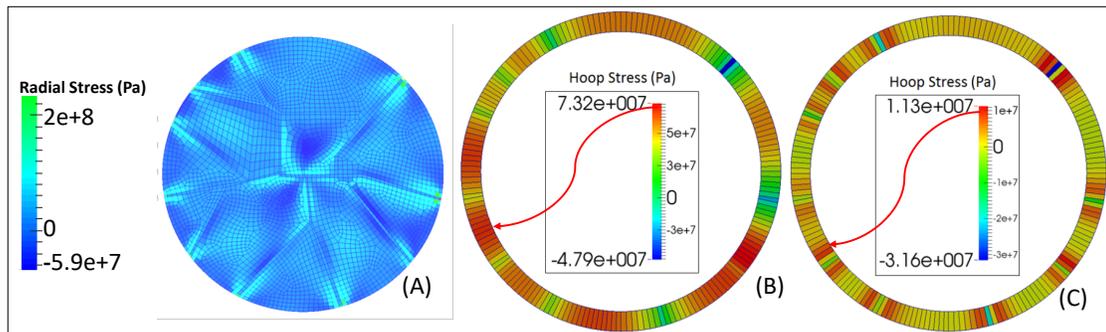


Figure 4. Stress distribution in bonded fuel for the case with 400°C peak temperature.

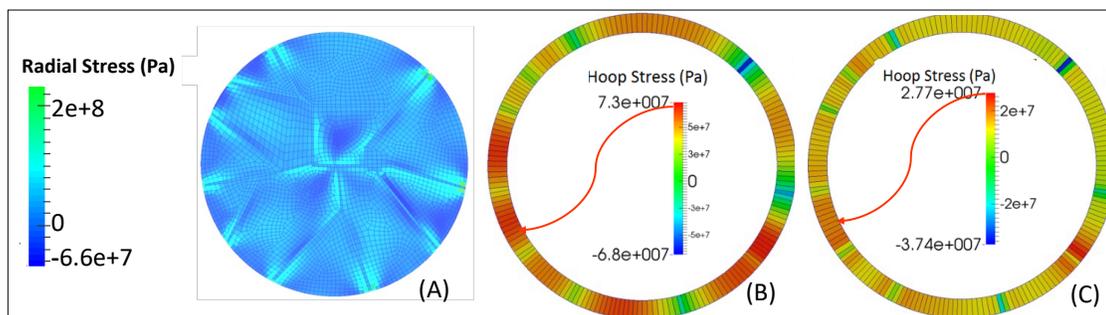


Figure 5. Stress distribution in bonded fuel for the case with 350°C peak temperature.

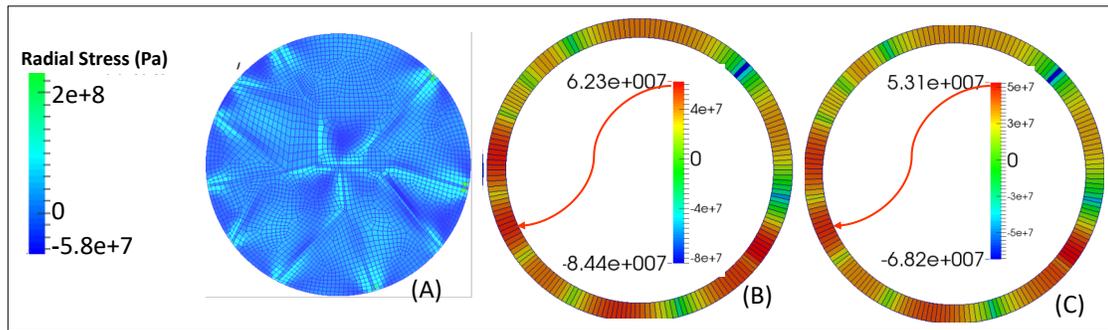


Figure 6. Stress distribution in bonded fuel for the case with 300°C peak temperature.

4. Sensitivity Analysis of Bond Breaking

The most likely condition for the bond to break is during shutdown and removal to 40°C wet storage. The time history analyses described in Section 3 include such shutdown events, but with the bond remaining intact. To help determine if debonding can occur and where it initiates from, Figure 7 was developed from the time history analyses of Section 3, which depicts radial stress distribution in the fuel at 40°C. This figure is examined next for evidence of debonding.

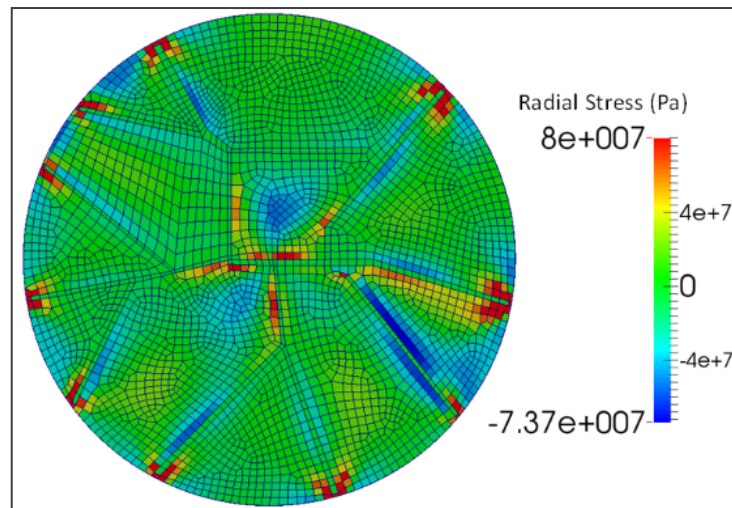


Figure 7. Radial stress distribution at 40°C obtained from the time-history analysis.

The bonding layer at the fuel-cladding interface is the result of diffusion bonding of the two materials UO_2 and ZrO_2 . The fracture strength of the bonding layer is conservatively assumed to be the lower of the two materials, which is 80 MPa at 40°C estimated from the MATPRO database for UO_2 [5]. The fuel-cladding bond is assumed to be broken when the stress is at or above the fracture strength of UO_2 . Evidence of potential bond breaking at 40°C is visible in Figure 7 in parts of the bonding layer at isolated locations near fuel cracks. The maximum value of the stress distribution shown in the figure is set to 80 MPa, the fracture strength of UO_2 at 40°C, to allow for better visualization of fuel-cladding debonding condition.

4.1 Description of Debonding Analysis Methodology

The debonding analysis methodology uses the FALCON code with 2D plane strain R- θ representation of the fuel rod shown in Figure 8. The analysis is aimed first at deriving a

debonding criterion for use in the fuel-cladding bonding model. The metrics used to detect debonding are a reduction in the fuel radial stress and/or an increase in the cladding hoop stress towards the pressurized open gap condition. However, the same effect, but to a lesser degree, would occur due to the formation of pressurized circumferential cracks in the interior part of the fuel. Thus, there is an interplay between fuel-cladding debonding and fuel circumferential cracking, as will be seen in the analysis results.

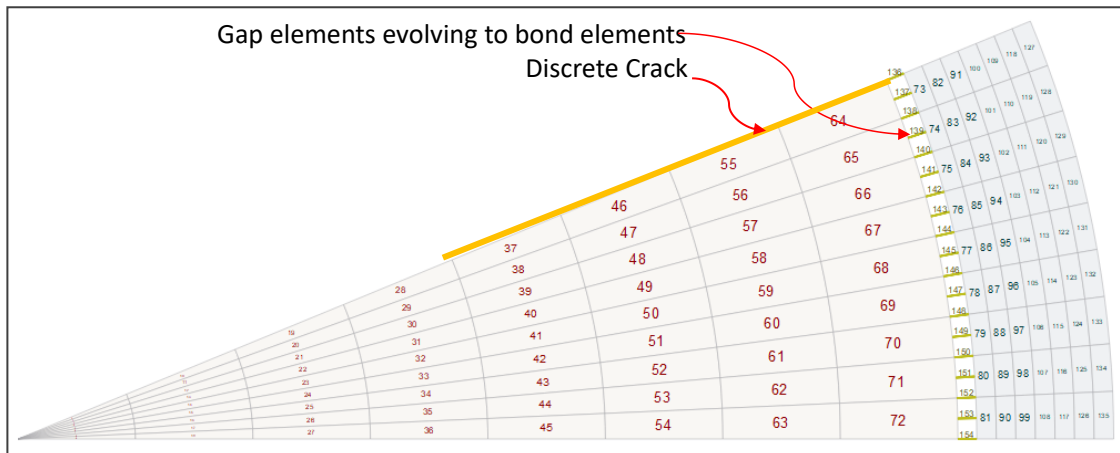


Figure 8. FALCON R-θ mesh for debonding analyses

The analysis was performed with the following initial conditions: Burnup of 55.0 GWd/MTU, fast fluence of $9.78 \times 10^{25} \text{ n/m}^2$ ($> 1 \text{ Mev}$), and gap ratio of 0.25. The gap ratio of 0.25 was selected so that gap closure can occur relatively early during the ramp to power. Four power cycles from hot zero power to full power of 25 kW/m were performed over a period of ~500 hours to activate cracking in the fuel pellet, followed by shutdown and wet storage for ~52 hours, then vacuum drying and constant temperature hold for ~376 hours. Fuel-cladding bonding was introduced in the 4th cycle at ~450 hours during full power operation, with gap closure in effect. The vacuum drying process was simulated by applying a constant decay power value of 1 W/m, corresponding to ~1 kW per assembly, and adjusting the cladding surface heat transfer coefficient to induce a cladding temperature increase from 40°C, the wet storage temperature, to 400°C within 24 hours, then held constant for 376 hours. The total simulation time is 1000 hours, as shown in Figure 9. The power history that produced the cyclic part of this temperature history would have similar shape.

Falcon analyses were performed using the finite element model shown in Figure 8 for three different power levels, 22 kW/m, 25 kW/m and 30 kW/m, each having four different trial values of bond strength, ranging from 92 MPa to 125 MPa, assigned to the gap/bond elements radial stress. Fuel-cladding interface elements 136 to 154, (see Figure 8), were assigned the same trial stress in each analysis run, but element 136 response was ignored because of stress concentration at that location due to its proximity to the discrete pellet crack. Based on the results of those trial analyses, a bond strength criterion of 110 MPa was selected.

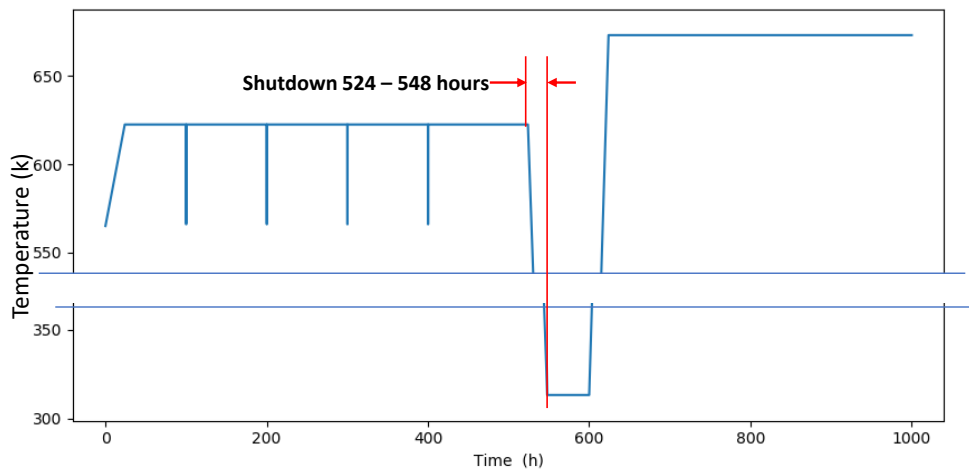


Figure 9 Cladding outer surface temperature history for FALCON R-θ simulations

4.2 Validation of Bond Strength Criterion

The 110 MPa bond strength was validated by repeating the analysis for the three power cases using 110 MPa as the debonding criterion. The analysis results indicated that the bond remained intact for the 22 kW/m and 25 kW/m cases but failed, as expected, for the 30 kW/m case. Figure 10 depicts the stress history for bond element 137 and cladding elements 73 and 74 which are closest to the pellet crack validating the 110 MPa bond strength. Note that in this analysis gap re-pressurization upon bond failure was not applied.

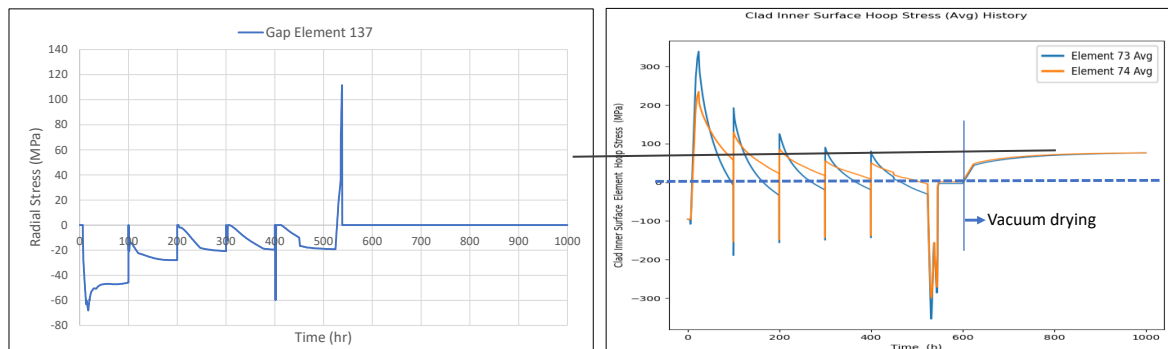


Figure 10 Validation analysis for bond strength criterion of 110 MPa showing bond element response (left) and cladding inner surface hoop stress (right) during power shutdown to 40°C from 30 kW/m.

4.3 Effects of Circumferential Cracks

The negative PCMI force in bonded fuel during power shutdown is affected by both the strength of the bond and the strength of the fuel matrix. Under certain conditions tenacious fuel-cladding bond can shift the failure tendency to the fuel matrix by forming circumferential cracks. Therefore, the fracture strength of UO₂ relative to the fuel-cladding bond strength becomes an important consideration in the present study. The UO₂ fracture strength, as a material property input to the smeared cracking model in Falcon, is defined by the equation below based on the MATPRO database [5]:

$$|\sigma_F = A(2.62D - 1.62)^{1/2} G^{-m} e^{-Q/RT}|$$

A = 170 MPa, original value (unirradiated)
 A = 85 MPa, updated value (irradiated UO₂)
 G = grain size (10⁻⁵m)
 D = Theoretical density fraction (0.95)
 R = gas constant (8.314 J/mol-K)
 m = 0.047
 Q = 1590 J/mol
 T = temperature (K)

Using A = 85 MPa for irradiated material, σ_F is calculated to be ~75 MPa and ~117 MPa for T=40°C and T=1000°C, respectively, the applicable temperature range in the present analysis, typical for 30 kW/m linear heat generation rate.

Repeating the case analysis represented in Figure 10 above, incorporating the above UO₂ fracture equation in Falcon's smeared cracking model, produced the results depicted in Figures 11, 12 and 13. Figure 11 shows the fuel element radial strain profile along a radial line bisecting the finite element model (elements 5, 14, 23, 32, 41, 50, 59, 68 in Figure 8) at different times during the shutdown phase shown in Figure 9. The strain profile in Figure 11 at element 23, with centroid located at about one third of the fuel radius exhibits circumferential crack evolution with smeared crack strain of 5.5%. All elements in the same radial position exhibit similar strain profile as element 23, indicating a complete circumferential crack.

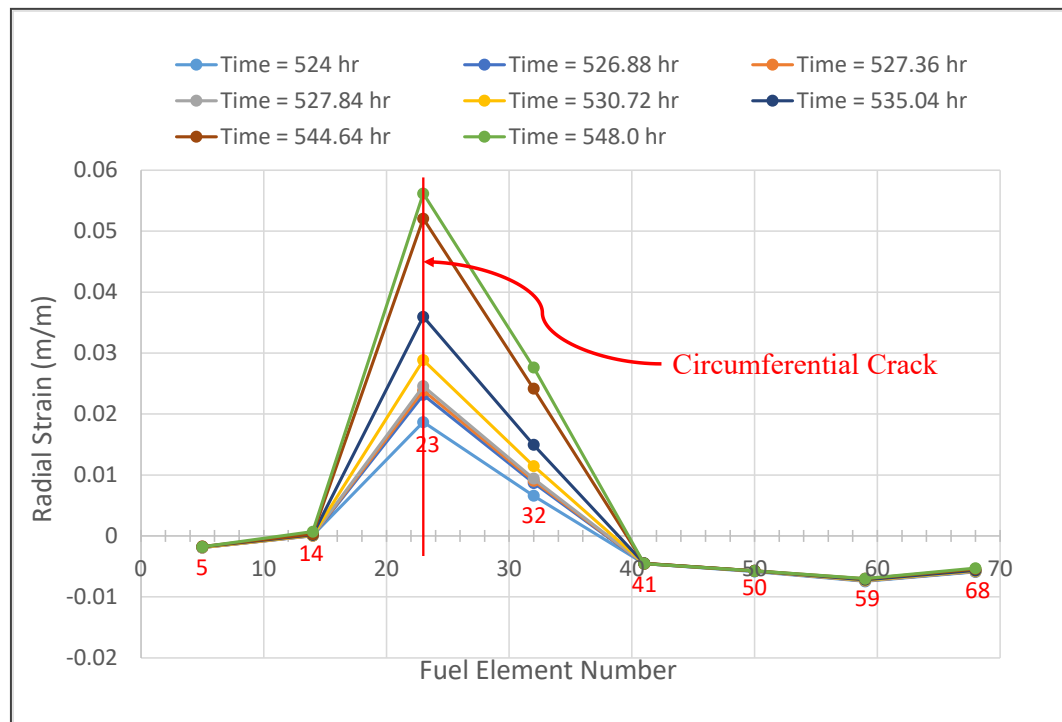


Figure 11. Fuel element radial strain along a radial line at various times during the shutdown phase

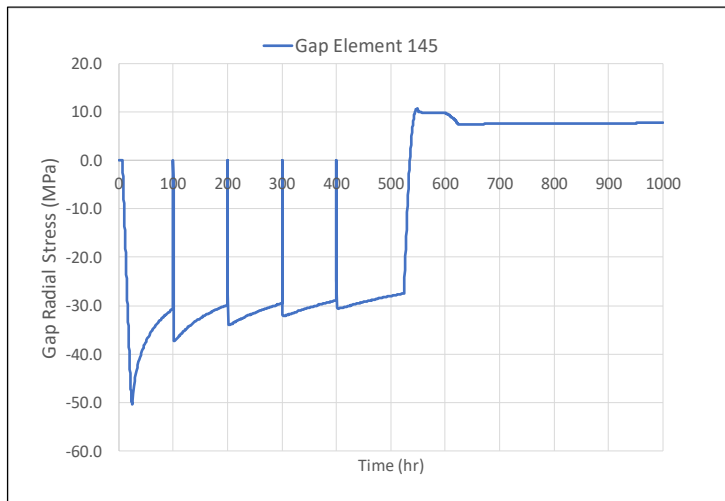


Figure 12. Radial stress in the gap/bond layer as a function of time

Figure 12 depicts the radial stress for gap/bond element 145, which is along the same radial line as the fuel element set. The tension in the gap element indicates that fuel-cladding bond remained intact preventing the fuel pellet from contracting freely. This behavior of impeded pellet contraction during cooling caused by unbroken bond is applying tension on the cladding, causing hoop compression as depicted in Figure 13, which shows the hoop stress for cladding elements 77 at the inner surface, 104 in the middle and 131 at the outer surface, which fall along the same radial line as the fuel element set. It is noted that the analysis was performed without applying system pressure on the outer surface of the cladding in order to delineate the effect of bond strength on cladding stress. This is clearly illustrated in Figure 13 which shows net compressive state of stress immediately upon shutdown to wet storage, (small tension on the outer surface and ~ -100 Mpa on the inner surface). During vacuum drying phase beginning at 600 hours the stress rose to become mainly tensile at ~ 60 Mpa on the outer surface relaxing to ~ 40 Mpa at 1000 hours.

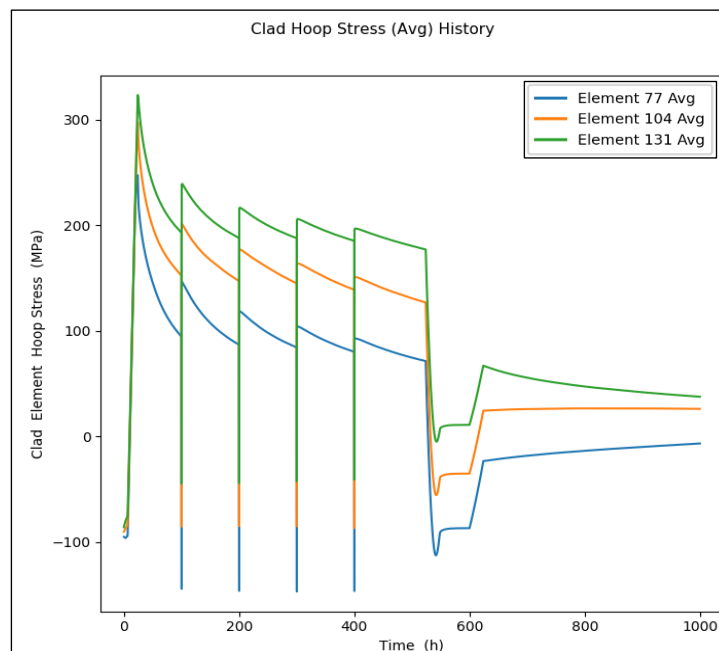


Figure 13. Cladding hoop stress: element 77 (inner surface), element 104 (midplane), element 131 (outer surface) as a function of time

5. Summary and Conclusion

The present study focuses on evaluating the effect fuel-cladding bonding could have on the behavior of the cladding during dry storage at peak temperatures less than 400°C and the conditions in which the pellet-cladding bonding becomes sensitive to breaking. The study examines the two questions: What is the effect of fuel-cladding bonding at peak cladding temperature lower than 400°C; and does pellet-cladding bonding in high burnup spent fuel remain intact during reactor shutdown and wet storage.

The overall results clearly indicate that high burnup spent PWR fuel rods with pellet-cladding bonding follow very different behavior regimes from the historical assumptions of pressurized empty tubes. The present analysis reveals several insights:

- Reducing initial storage temperature does not necessarily lead to lower stresses.
- Creep is found to be highly beneficial for PCT of 400°C, slightly beneficial for PCT of 350°C, and not very beneficial for PCT of 300°C.
- The 400°C condition in Reference [1] results in lower radial hydride concentration compared to the 350°C and 300°C condition.
- Pellet-cladding debonding condition can develop but remains localized over one or two millimeters at pellet cracks.
- Fuel-cladding bond once formed in high burnup fuel remains intact throughout the entire fuel cycle, including the backend.
- Circumferential cracks can form during shutdown, especially in fuel with high power operating history. These circumferential cracks can cause a fuel layer to participate in resisting internal-pressure loading, resulting in much reduced cladding hoop stress. The closer the circumferential crack to the fuel OD, the thinner the bonded fuel layer and the higher the cladding hoop stress.
- An assumed broken bond over a 27-degree sector, (7.5% of the cladding circumference), would be sufficient to simulate empty tube behavior. However, the fact that the fuel-cladding bond is highly resistant to breaking, the likelihood of such hypothetical case existing is small.

6. References

- 1) W. Lyon, A. Mai, W. Liu, N. Capps, J. Rashid, A. Machiels, K. Waldrop, "Impact of Fuel-Cladding Bonding on the Response of High Burnup Spent Fuel Subjected to Transportation Accidents", 2018 Top Fuel Conference.
- 2) Impact of Fuel-Cladding Bonding on the Response of High Burnup Spent PWR Fuel Subjected to Dry Storage and Transportation Accidents, EPRI-3002015075, 2019.
- 3) Evaluation of Fuel-Cladding Debonding Conditions on the Response of High Burnup Spent PWR Fuel Subjected to Dry Storage and Transportation Accidents, EPRI-3002020527, April 2021.
- 4) J. Machiels et. al., "Characterization of end-of-life rod internal pressure in PWR fuel", Nuclear Engineering and Design, Volume 324, 1 December 2017, Pages 250-259.
- 5) SCDAP/RELAP5-3D Code Manual Volume 4: MATPRO – A Library of Materials Properties for Light Water Reactor Accident Analysis, INEEL/EXT-02-00589 Volume 4 Revision 2.2, October 2003.
- 6) Fuel Analysis and Licensing Code: FALCON MOD01: Volume 1: Theoretical and Numerical Bases. EPRI, Palo Alto, CA: 2004. 1011307
- 7) Hales, J.D., K. A. Gamble, B. W. Spencer, S. R. Novascone, G. Pastore, W. Liu, D. S. Stafford, R. L. Williamson, D. M. Perez, R. J. Gardner, BISON User's Manual: BISON Release 1.2, Technical Report INL/MIS-13-30314 Rev. 2, Idaho National Laboratory, September 2015.